scientific reports

Check for updates

OPEN

Identification of small ubiquitin-related modifier (SUMO)-related genes-based biomarkers in Alzheimer's disease based on bioinformatics analysis

Peng Chen[1,4], Mengting Fan[2,4], Hailiang Lin[2], Zhong Chen[2], Qiuyang Zhang[2], Yunfan Cheng[1] & Jing Xu[3]✉

To investigate the role of small ubiquitin-like modification (SUMO) in Alzheimer's disease (AD) and its pathogenesis, this study employed bioinformatics methods to identify diagnostic biomarkers for AD based on SUMO-related genes (SRGs). It further conducted preliminary explorations into their role in AD pathogenesis and potential therapeutic targets. Datasets related to AD (GSE140831, GSE63060), a dementia dataset (GSE140830), and 189 SRGs were retrieved from public databases. Candidate genes were identified by intersecting differentially expressed genes (DEGs) with SRGs. A protein–protein interaction (PPI) network was constructed to select the top 15 core genes, and the support vector machine-recursive feature elimination (SVM-RFE), least absolute shrinkage and selection operator (LASSO) and boruta random forest (Boruta-RF) identified feature genes. Validation was done using the GSE140831 and GSE63060 datasets, and the nomogram model was assessed by receiver operating characteristic (ROC) curve analysis. Gene set enrichment analysis (GSEA) and other analyses were performed. Reverse transcription quantitative polymerase chain reaction (RT-qPCR) was used for further validation. Overlapping 189 SRGs and 12,853 DEGs identified 107 candidate genes. Six overlapping genes were selected. *CREBBP*, *PIAS1*, and *TRIM28* were confirmed as AD biomarkers due to their increased expression in AD and strong ROC performance. GSEA highlighted their involvement in pathways such as olfactory transduction, lysosome, and spliceosome. Immune infiltration analysis suggested immune cell involvement in AD progression. Additionally, 21 potential drugs for AD therapy were predicted. RT-qPCR confirmed the over-expression of CREBBP and TRIM28 in AD samples, consistent with dataset trends. *CREBBP*, *PIAS1*, and *TRIM28* were identified as SRG-based biomarkers for AD diagnosis, providing new insights into AD pathogenesis.

Keywords Alzheimer's disease, Small ubiquitin-related modifier-related genes, Bioinformatics analysis, Biomarkers

Alzheimer's disease (AD) is the most common neurodegenerative disease worldwide, with progressive cognitive decline as the main clinical feature[1]. Alzheimer's Association International estimated there are around 50 million people with dementia worldwide, which is expected to triple by 2050[2]. The main manifestations of AD are progressive cognitive impairment and personality disorder[3]. The APOE gene is the most common risk gene for AD[4]. Deposition of amyloid beta (Aβ) in the brain parenchyma and cerebrovascular system, as well as the presence of neurofibrillary tangles within neurons and progressive loss of synapses, are central neuropathological markers of AD[5]. Current drug treatments of AD only have symptomatic effects, and there is no treatment to alleviate the disease[6], so new advances in the diagnosis and treatment of AD remain an urgent task. The search for biomarkers of AD is of great significance in further promoting AD treatment.

[1]Department of Geriatrics, Fuzhou Second General Hospital, Fuzhou, China. [2]Department of Neurology, Fuzhou Second General Hospital, Fuzhou, China. [3]Department of Endocrinology, Fuzhou Second General Hospital, 47 Shangteng Road, Fuzhou, China. [4]Peng Chen and Mengting Fan are the co-first authors ✉email: xujinghe-6ren@163.com

Small ubiquitin-related modifier (SUMO), a 97-residue protein, mediates post-translational modification through covalent attachment to a specific lysine residue on the target protein[7]. Ubiquitination plays a important role in the biochemical pathways of eukaryotes by influencing the location, function, and stability of modified proteins[8]. In histopathology, AD is characterized by the insoluble aggregation of Aβ and microtubule-associated protein tau in the brain, both of these proteins are associated with SUMO. It has been demonstrated that tau SUMOylation reciprocally promotes its hyperphosphorylation, which results in aggregation of tau to form neurofibrillary tangles, and eventually interferes with the normal function of neurons and leads to nerve cell death[9]. And early studies have indicated that the SUMO system may impact Aβ levels and tau aggregation by altering with AD-type pathology[10]. Among these, SUMO-2 can inhibit the conversion of Aβ into β-sheet structures and impede its aggregation[11]. Meanwhile, specific single nucleotide polymorphisms (SNPs) in the SUMO1/2 genes have been confirmed to be associated with the genetic risk of Alzheimer's disease in the Korean population[12]. At the level of aging mechanisms, telomere length is closely linked to biological aging, and recent studies have demonstrated an association between telomere attrition and the onset of AD[13]. Accumulating evidence indicates that the ubiquitin and SUMO pathways, as key regulators of the telomere protection complex and other chromatin modifiers, are crucial for maintaining telomere structural integrity[14]. However, current studies predominantly focus on individual molecular mechanisms or genetic associations, lacking exploration of the overall transcriptional regulatory network of SUMO-related genes (SRGs) in AD. Moreover, a clinically applicable biomarker system based on SRGs has yet to be developed. Therefore, investigating SRG-based diagnostic biomarkers for AD and elucidating the mechanisms by which these factors influence AD are of significant importance for improving interventions in AD patients and providing new directions for AD treatment.

Based on an AD-related dataset (GSE140831) and 189 SRGs, this study screened candidate genes and, through machine learning algorithms, differential expression analysis, and functional enrichment analysis, identified SUMO-related genes associated with AD. Further validation was conducted to assess their potential as diagnostic biomarkers. On this basis, the study not only constructed a nomogram model for AD risk prediction but also performed multi-dimensional exploration, including enrichment analysis, immune infiltration analysis, and drug prediction. These approaches preliminarily revealed the potential functional mechanisms and regulatory networks of these genes in AD pathogenesis, thereby providing new research clues for the early diagnosis, mechanistic interpretation, and discovery of therapeutic targets for AD.

Materials and methods

Data collection

The expression profiles of GSE140831 (GPL15988), GSE63060 (GPL6947), and GSE140830 (GPL15988) datasets were searched from the Gene Expression Omnibus (GEO) database (http://www.ncbi.nlm.nih.gov/geo/)[15]. Specifically, 734 peripheral blood samples from 204 patients with AD and 530 healthy persons (controls) in the GSE140831 dataset were selected as a training set. The GSE63060 dataset offered peripheral blood samples from 145 AD and 104 controls. Besides, the GSE140830 dataset was composed of peripheral blood samples from 261 dementia patients (80 of behavioral variant frontotemporal dementia (bvFTD), 44 in semantic variant primary progressive aphasia (svPPA), 47 from non-fluent variant primary progressive aphasia (nfvPPA), 54 of progressive supranuclear palsy (PSP) and 36 of corticobasal syndrome (CBS) and 281 controls. A sum of 189 small ubiquitin-related modifiers (SUMO) related genes (SRGs) was retrieved from the Molecular Signatures Database (MSigDB, https://www.gsea-msigdb.org/) as 'SUMOylation' being a keyword. The research workflow is presented in Online Resource 1.

Differential expression and functional enrichment analyses

The differentially expressed genes (DEGs) of AD between AD and control groups in the GSE140831 dataset were obtained employing the R package 'limma' (Ver. 3.54.1)[16](|Log_2fold-change (FC)|> 0.1, adjusted $p < 0.05$). Subsequently, utilizing the R package 'ggVenndiagram' (Ver. 1.2.2)[17], the candidate genes associated with AD and SRGs were acquired through intersecting observably up-regulated and down-regulated DEGs with SRGs, respectively. Subsequently, the relevant functions and signaling pathways in which candidate genes were involved were investigated via Gene Ontology (GO) and Kyoto Encyclopedia of Genes and Genome (KEGG)[18,19], implemented with the R package 'clusterProfiler' (Ver. 4.6.2)[20] (adj $p < 0.05$). Additionally, a protein–protein interaction (PPI) network revealing interactions among proteins encoded by candidate genes was built and visualized by the Search Tool for Recurring Instances of Neighboring Genes database (STRING, https://string-db.org) (Interaction score = 0.4) and the plug-in CytoHubba of Cytoscape software severally (Ver. 3.9.0)[21]. The TOP 15 candidate genes in the PPI network were singled out as core genes for screening biomarkers.

Acquisition of the biomarkers and construction of a nomogram model

To identify biomarkers for the detection and diagnosis of AD, this study employed three machine learning approaches for feature gene selection: the Least Absolute Shrinkage and Selection Operator (LASSO), Boruta Random Forest (Boruta-RF), and Support Vector Machine Recursive Feature Elimination (SVM-RFE). Specifically, using the R package "e1071" (Ver. 1.7–13)[22]to perform tenfold cross-validation. Feature genes selected by the Support Vector Machine-Random Forest (SVM-RF) model were extracted from the core genes when the model achieved the highest accuracy and lowest error rate. LASSO regression analysis was implemented using the "glmnet" package (Ver. 4.1–8)[23], with alpha set to 1, family set to binomial, and tenfold cross-validation employed to determine LASSO feature genes. Boruta-RF analysis employed the "Boruta" package (Ver. 8.0.0)[24] with parameters maxRuns = 100 and doTrace = 0. Additionally, the mean area under the receiver operating characteristic curve (AUC) and its standard deviation were calculated for each method under tenfold cross-validation to quantify predictive performance. Concurrently, overlapping genes were identified based on gene

overlap across the three machine learning algorithms. Subsequently, the expression verification of feature genes in the GSE140831 and GSE63060 datasets proceeded to ascertain genes with observably discrepant expression levels in AD and control groups and consistent expression trends in the two datasets as the biomarkers for AD. Wilcoxon's test estimated the significantly different expression levels of inter-group feature genes ($p < 0.05$). Furthermore, based on the GSE140831 dataset, a nomogram model predicting the risk of AD was established through the R package 'rms' (Ver. 6.5–0)[25]. The nomogram model could visualize a total point for each sample in the GSE140831 dataset, and the risk of AD grew along with the increased total points. Receiver operating characteristic curves were plotted using the R package pROC (version 1.18.0)[26]. The predictive performance of the predictive mapping model constructed in this study, as well as that of individual biomarkers, was evaluated by calculating the AUC.

Gene set enrichment analysis (GSEA)

To explore whether biomarkers were involved in regulating the progression of AD, the underlying pathways enriched by them were defined via GSEA. The Spearman's correlation coefficients between biomarker and other genes in the GSE140831 dataset were calculated adopting the R package 'psych' (Ver. 2.2.9)[27]and queued in order, and the sorted genes were input into the 'clusterProfiler' package in R to match relevant pathways of biomarkers (adj.$p < 0.05$, $|NES| > 1$).

Construction of molecular regulatory network

The prediction of upstream molecules targeting biomarkers was beneficial in understanding the biological functions of biomarkers. So, the transcription factors (TFs) regulating biomarkers were predicted via the NetworkAnalyst (http://www.networkanalyst.ca) database. Moreover, the microRNAs (miRNAs) retrieved from the miRWALK (http://mirwalk.umm.uni-heidelberg.de/) and miRDB (http://www.mirdb.org) databases were overlapped as miRNAs corresponding to biomarkers. The feat of the Cytoscape software synthesized the TF-mRNA and miRNA-mRNA networks.

Immunoinfiltration characterization and drug prediction

To characterize the discrepancies in immune cell infiltration between AD and control groups, the abundance of 64 kinds of immune cells in each sample of the GSE140831 dataset was estimated through the xCell algorithm[28]. The discrepant immune cells in the AD and control groups were found through Wilcoxon's test ($p < 0.05$). Ulteriorly, Spearman's correlation analysis uncovered associations among discrepant immune cells and between discrepant immune cells and each biomarker ($|cor| > 0.4$, $p < 0.05$).

Moreover, the Drug-Gene Interaction Database (DGIdb, www.dgidb.org) identified feasible drugs targeting biomarkers for AD therapy, and a gene-drug network was created through Cytoscape software.

Assessment of expression levels of biomarkers in the five dementia-related diseases

To understand the expression of biomarkers in five dementia-related diseases (bvFTD, svPPA, nfvPPA, PSP, and CBS), the expression patterns of the biomarkers in AD and control groups were first displayed in a heatmap plotted by the R package 'ggplot2' (Ver. 3.3.6)[29]. Besides, the differences in the expression of biomarkers in five dementia-related diseases were compared through Wilcoxon's test ($p < 0.05$).

Real-time reverse transcriptase-polymerase chain reaction (RT-qPCR)

The RT-qPCR was the assay of choice for detecting relative biomarker expression levels in five pairs of AD and control whole blood samples gathered from Fuzhou Second General Hospital. All whole blood samples were collected in the morning under fasting conditions. Approximately 2 ml of peripheral venous blood was drawn from each participant using EDTA anticoagulant tubes and immediately stored at −80 °C for subsequent analysis. All sample donors signed the informed consent forms. This study was conducted in accordance with the Declaration of Helsinki and obtained ethical approval from the Ethics Committee of Fuzhou Second People's Hospital (Approval No.: 2024005). The total RNA was extracted from the ten samples using the TRIzol reagent (Ambion, USA) per the manufacturer's protocol. The concentrations of total RNA were detected in rapid sequence via the NanoPhotometer N50. Ulteriorly, the cDNA synthesis was reverse-transcribed using the SureScript-First-strand-cDNA-synthesis-kit (Servicebio, China). Additionally, the CFX Connect Thermal Cycler (Bio-Rad, USA) was operated to detect the relative expression level of mRNA using the GAPDH as an internal reference gene for RT-qPCR through the $2^{-\Delta\Delta CT}$ method. The details of all primers are attached in Online Resource 2 which can be found in the supplementary file.

Statistical analysis

Bioinformatics analysis was implemented through this study's R software (Ver. 4.3.2). The Wilcoxon's test was used to distinguish the inter-group discrepancies, and a p-value or adj. p-value of less than 0.05 was deemed statistically significant.

Results

The functions of candidate genes might be related to nucleic acid and cytoplasmic transport and cancer regulation

12,853 DEGs were identified between the AD and control groups in the GSE140831 dataset (Fig. 1a). 107 candidate genes related to AD and SRGs, with 85 up-regulated and 22 down-regulated, were obtained by overlapping 189 SRGs and 6,640 up-regulated and 6,213 down-regulated DEGs (Fig. 1b-c). They were enriched in 624 GO entries, comprising 498 biological processes (BPs), 44 cellular components (CCs), and 82 molecular functions (MFs). Moreover, the functions of candidate genes were associated with nucleic acid transport,

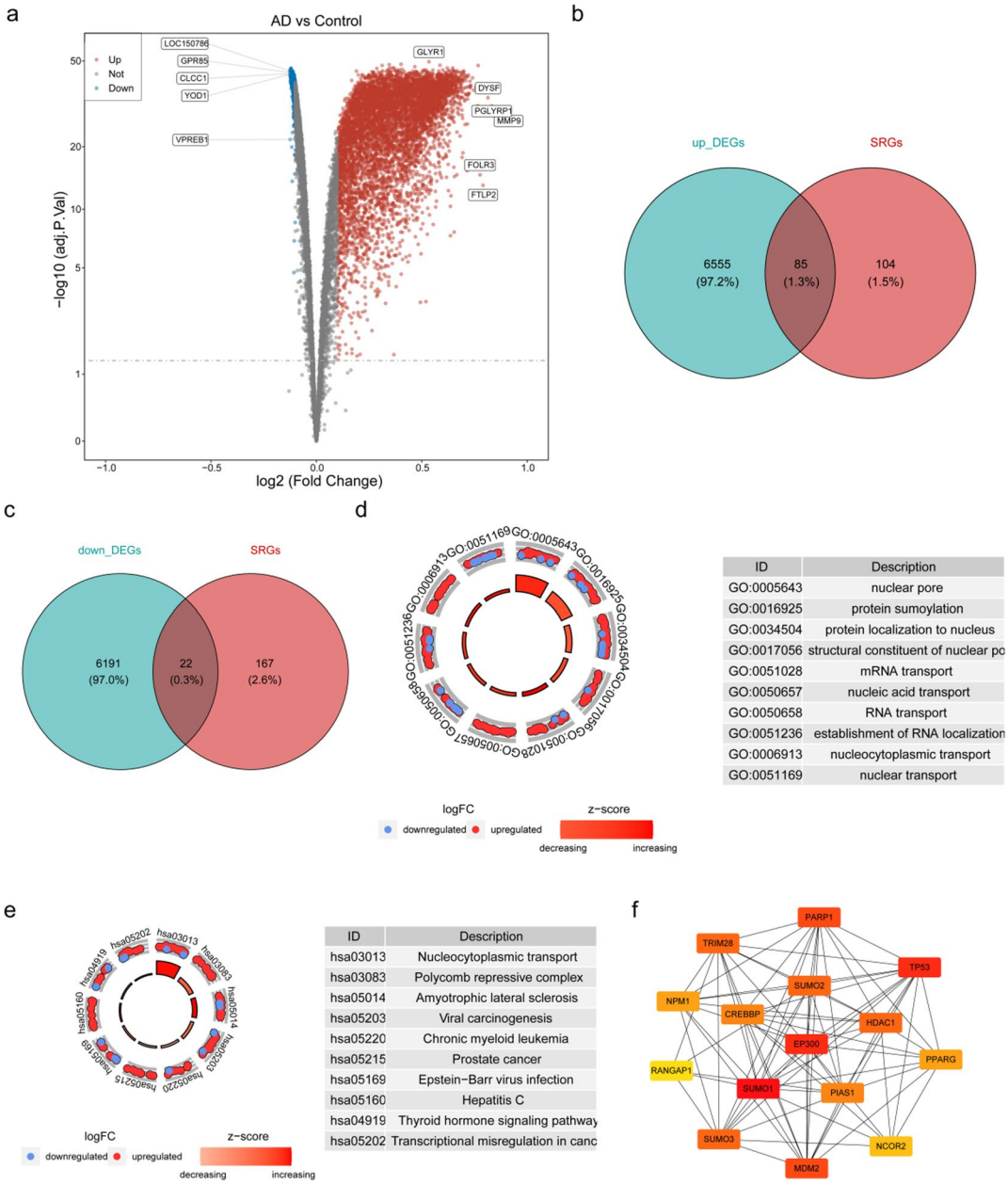

Fig. 1. Differential expression of genes (**a**) Volcano plot of differentially expressed genes between Alzheimer's disease (AD) and normal groups. Red dots represent upregulated genes, and blue dots represent downregulated genes. (**b**) Intersection of significantly upregulated genes and SUMOylation-related genes. (**c**) Intersection of significantly downregulated genes and SUMOylation-related genes. (**d**) Gene ontology (GO) enrichment analysis of candidate genes. Blue dots represent downregulated genes, and red dots represent upregulated genes. The red box in the middle indicates the degree of enrichment, with higher levels indicating greater enrichment. (**e**) Kyoto Encyclopedia of Genes and Genomes (KEGG) pathway enrichment analysis of candidate genes. Blue dots represent downregulated genes, and red dots represent upregulated genes. The red box in the middle indicates the degree of enrichment, with higher levels indicating greater enrichment. (**f**) Protein–protein interaction (PPI) network of candidate genes.

nucleocytoplasmic transport, protein sumoylation, and so on (Fig. 1d). Concerning the 34 KEGG pathways involved by candidate genes, they included not only cytoplasmic transport but also nucleocytoplasmic transport, transcriptional misregulation in cancer, chronic myeloid leukemia, etc. (Fig. 1e). Generally, 107 candidate genes might participate in nucleic acid and cytoplasmic transport and cancer regulation. Additionally, the PPI-based screening manifested that the interactions among 15 core genes, *PARP1*, *TRIM28*, *NPM1*, *RANGAP1*, *SUMO3*, *MDM2*, *NCOR2*, *PPARG*, *TP53*, *SUMO2*, *CREBBP*, *HDAC1*, *EP300*, *SUMO1* and *PIAS1*were close at protein level, especially among TP53, EP300 and SUMO1 (Fig. 1f).

The performance of the biomarker-based nomogram model in predicting the risk of AD was reliable

There were five feature genes (*CREBBP*, *PIAS1*, *TRIM28*, *MAD2*, and *NCOR2*) in the SVM-RFE model when the model had the highest accuracy (Fig. 2a). The LASSO model selected seven genes based on the optimal λ value: SUMO1, MDM2, NPM1, CREBBP, PIAS1, TRIM28, and NCOR2 (Fig. 2b). The Boruta-RF model identified twelve genes: SUMO1, SUMO2, SUMO3, MDM2, EP300, NPM1, CREBBP, PIAS1, RANGAP1, TRIM28, NCOR2, and PPARG (Fig. 2c). Notably, all three models demonstrated favourable discriminatory capabilities, with AUC values exceeding 0.7 (Online Resource 3a). By taking the intersection of the three models' screening results, six overlapping genes were identified (Fig. 2d). Among these, CREBBP, PIAS1 and TRIM28 were served as biomarkers for AD as a consequence of their observably increased expression levels in AD group and consistent expression trends in GSE140831 and GSE63060 datasets ($p < 0.05$) (Fig. 2e). The nomogram model created by absorbing three biomarkers demonstrated that the risk of AD increased with the total points corresponding to each sample in the GSE140831 dataset (Fig. 2f). The precise predictive performance of the nomogram model must be further confirmed by the AUC value of 0.809 (Fig. 2g). Moreover, three biomarkers also demonstrated predictive value, with their AUC values all exceeding 0.7 (Online Resource 3b).

Three biomarkers were involved in identical pathways, such as olfactory transduction, lysosome, and spliceosome

Exploring three biomarkers by GSEA was essential for understanding their effects on AD. The findings of GSEA unveiled that *CREBBP*, *PIAS1*, and *TRIM28* gathered in olfactory transduction, lysosome, and spliceosome were significantly and synchronously. Besides, Huntington's disease and neuroactive ligand receptor interaction were involved by *PIAS1* and *TRIM28*. In conclusion, GSEA certifies that three biomarkers might retain similar functions in regulating AD's progression (Fig. 3a-c).

The expression of three biomarkers was regulated by multiple TFs and miRNAs

How upstream molecules regulated three biomarkers was further explored; 58 TFs and 284 miRNAs targeted three. The TF-mRNA displayed that three biomarkers could be regulated by *EGR1*, *DMRT1*, *E2F1*, *CREM*, and *ZFX* simultaneously (Fig. 3d). In addition, as presented in Fig. 3e, the transcription of *TRIM28* and *CREBBP* could be regulated by hsa-miR-6812-5p, hsa-miR-1227-5p, and hsa-miR-7113-5p synchronously, as well as *CREBBP* and *PIAS1* by hsa-miR-4452, hsa-miR-1284, hsa-miR-6883-3p, and so forth.

Most of the immune cells might influence the progression of AD

Among the 64 immune cells, a total of 55 immune cells showed markedly discrepant abundance between the AD and control groups ($p < 0.05$). For instance, AD's percentages of basophils, class-switched memory B cells, myocytes, and mesenchymal stem cells (MSCs) were higher. In contrast, the proportions of natural killer T (NKT) cells, B cells, neutrophils, smooth muscle, and naive CD8(+) T cells were inverse in AD (Fig. 4a). Furthermore, Spearman's correlation analysis among discrepant immune cells uncovered that memory B cells and B cells maintained the highest positive correlations of 0.76 ($p < 0.05$), yet T helper type 1 (Th1) cells and neurons kept the highest negative correlations of -0.72 ($p < 0.05$) (Fig. 4b). Basophils were positively correlated with *PIAS1* and *CREBBP*, and myocytes with *TRIM28*. Besides neutrophils and *CREBBP*, *PIAS1* maintained significantly negative correlations, as well as smooth muscle and *TRIM28* ($|cor| > 0.4$, $p < 0.05$) (Fig. 4c-e).

A sum of 21 alternative drugs might be developed for AD therapy

What is more, a total of 21 drugs targeting *CREBBP* were retrieved in DGIdb, such as triazolam, colchicine, alprazolam, nocodazole, etc. (Fig. 4f, Online Resource 4). Unfortunately, no drugs targeting *TRIM28* and *PIAS1* were found in this database. Among these, triazolam and alprazolam were proven to be therapeutic for AD. However, applying them in large doses could produce side effects such as decreased blood pressure and respiratory circulation suppression, so drug prediction targeting biomarkers might provide data for developing available drugs for AD.

The expression level of TRIM28 was significantly increased in svPPA

The expression patterns of three biomarkers in five dementia-related diseases were exhibited in the heat map (Fig. 5a). Expression analysis of biomarkers confirmed that *CREBBP* and *PIAS1* showed no significant discrepancies between bvFTD, svPPA, nfvPPA, PSP, and CBS and controls, except for *TRIM28* with upregulated expression levels in svPPA (Fig. 5b-f).

CREBBP and TRIM28 were all over-expressed in AD samples

Consistent with the expression trend in the GSE140831 and GSE63060 datasets, the relative expression levels of *CREBBP* ($p = 0.0043$) and *TRIM28* ($p = 0.0032$) were increased in AD samples. While the expression level of *PIAS1* was not significant ($p > 0.05$) (Fig. 6a-c).

Discussion

Alzheimer's disease (AD) is a degenerative disease of the nervous system. Whose primary genetic risk factor is the APOE gene and is characterized by insoluble aggregation of proteins such as amyloid-beta (Aβ)[30]. As A post-translational modification, SUMOylation has been shown to regulate multiple cellular pathways. SUMO is believed to be closely related to key proteins in AD, such as Aβ and the microtubule-associated protein tau, and is involved in regulating various cellular functions associated with AD pathology[31]. In addition, the SUMO pathway is also associated with AD's occurrence and development by affecting the telomere structure's integrity, which can provide a new research perspective for diagnosing and treating AD[32,33]. However, bioinformatic analysis of

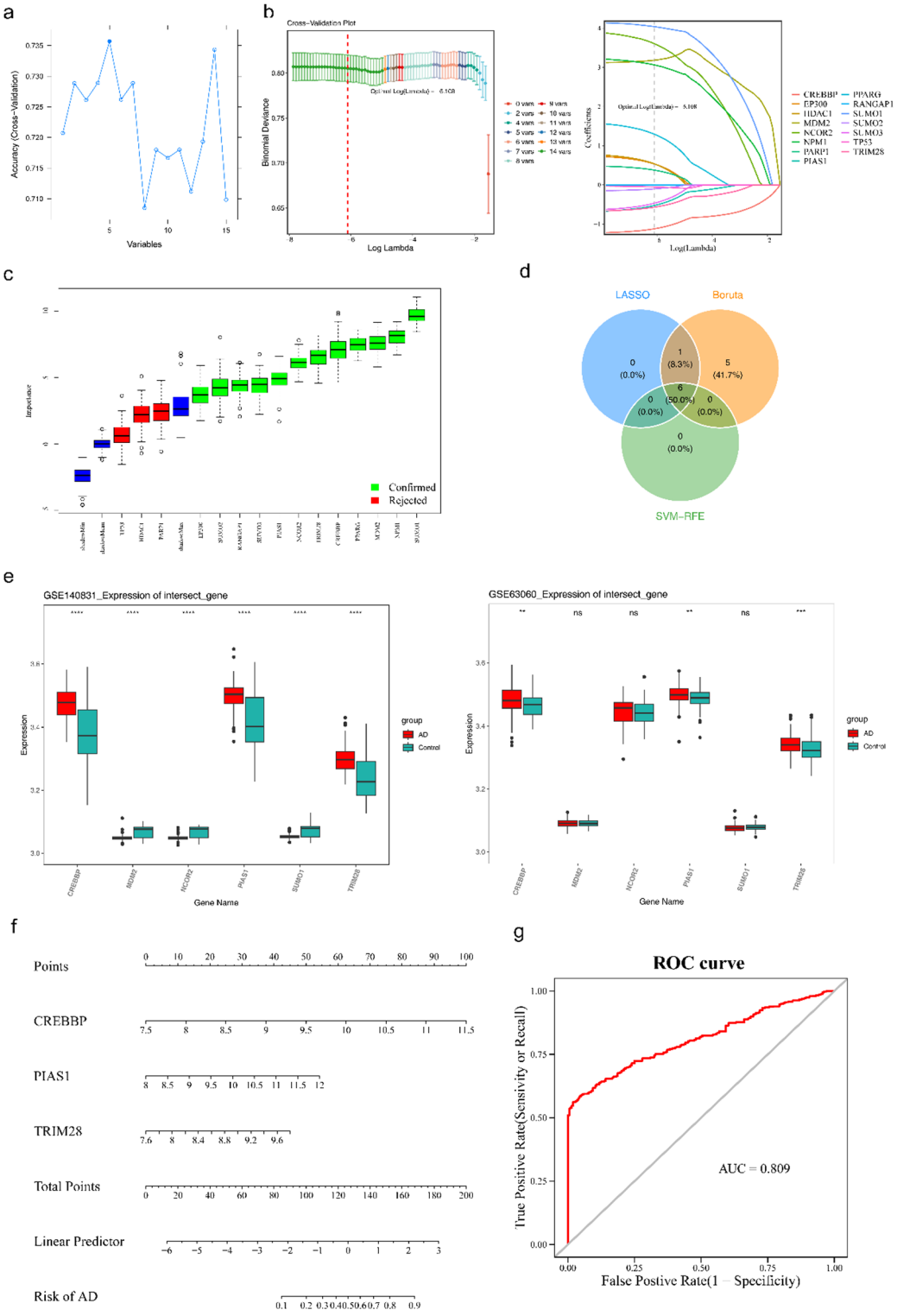

Fig. 2. Biomarker screening and nomogram construction (**a**) Results of feature selection using the SVM-RFE algorithm. The error rate of the support vector machine model is shown. (**b**) Results of feature selection using the LASSO algorithm. (**c**) Results of feature selection using the Boruta-RF algorithm. (**d**) Screening results from the three models were integrated using Venn diagrams. (**e**) Expression validation analysis of feature genes in the training set and validation set. Red represents the AD group, and green represents the normal group. ****, $p < 0.0001$; **, $p < 0.01$; ns, not significant. (**f**) Nomogram based on biomarkers. (**g**) ROC validation of the nomogram.

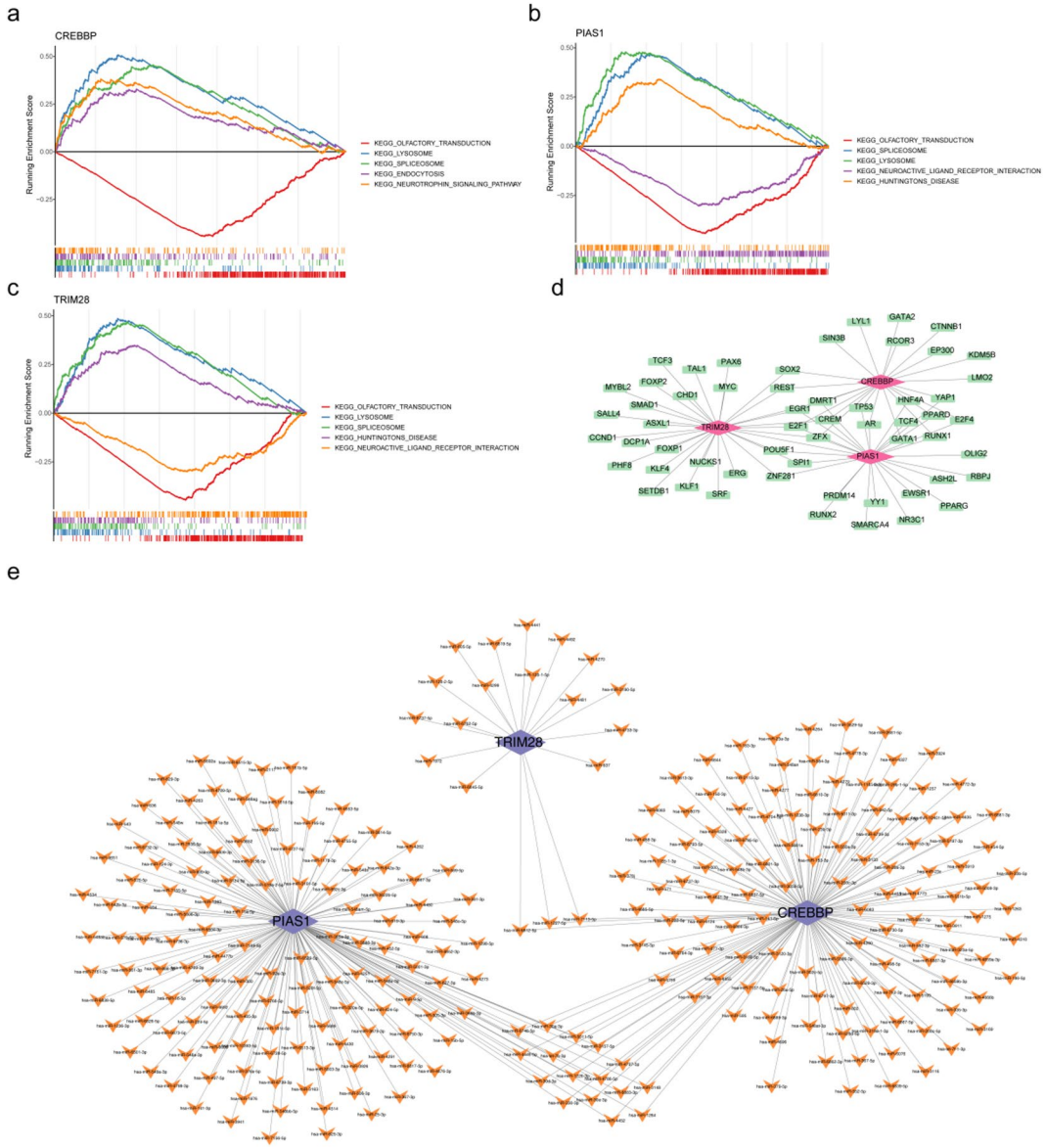

Fig. 3. Enrichment analysis of biomarkers and construction of related networks (**a**-**c**) GSEA analysis of biomarkers. The y-axis represents the enrichment score, and the x-axis represents genes, with each vertical line representing a gene. (**a**) CREBBP. (**b**) PIAS1. (**c**) TRIM28. (**d**) Biomarker-transcription factor network. Red nodes represent mRNAs (biomarkers), and green nodes represent transcription factors. (**e**) Biomarker-MicroRNA network. Purple nodes represent mRNAs (biomarkers), and orange nodes represent MicroRNAs.

SRGs in AD has not yet been performed, and crucial SRG-based biomarkers involved in the pathogenesis of AD have not been confirmed.

In the present study, we identified the SRGs associated biomarkers in AD based on the GSE140831, GSE63060, and GSE140830 datasets, specifically *CREBBP*, *PIAS1*, and *TRIM28*. These biomarkers are potential diagnostic targets for AD because of their increased expression levels in the AD group and reliable predictive performance. GSEA and the prediction results of TFs suggest that these biomarkers may have similar biological functions in AD's progression, and the expression of three biomarkers could be regulated simultaneously by some TFs. Immune infiltration analysis suggested that, between the AD and control groups, the proportion of specific immune cells correlated significantly with these biomarkers. Finally, we speculate a total of 21 drugs as potential therapeutic agents for AD on DGIdb, in addition to triazolam and alprazolam, which have been used in the treatment of AD.

CREBBP is a transcriptional coactivator with histone acetyltrans-ferase (HAT) activity and is involved in post-translational modification by acetylation of histones[34], there are studies showed that dysregulation of histone acetylation pathways is thought to play may play a key role in the disease progression of AD. Hence, dysfunction of *CREBBP* is likely to contribute to neurodegenerative diseases[35,36]. In addition, recent studies have shown that *CREBBP* may be a hub gene that provides new insight into treating AD by mediating the metabolism

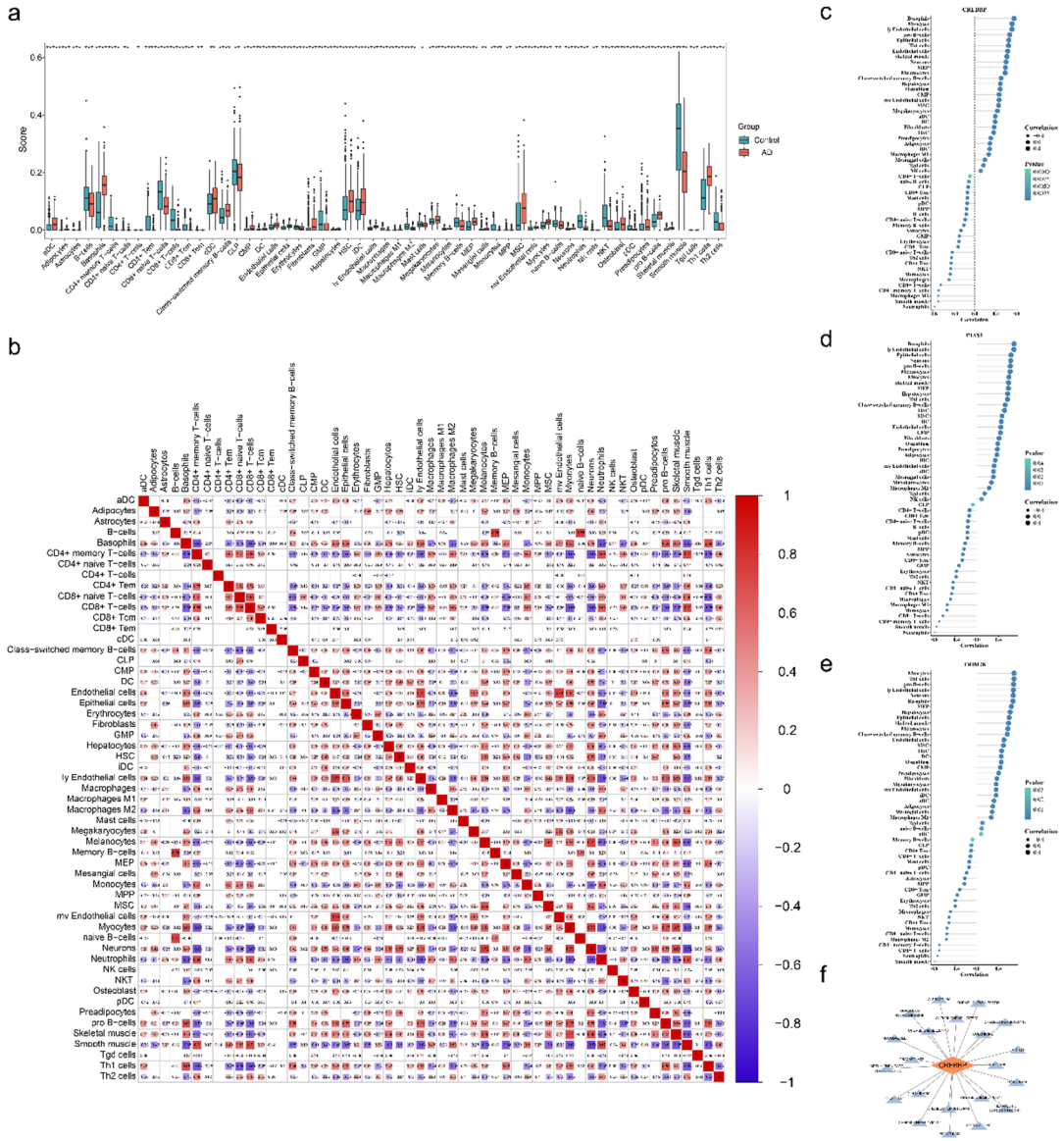

Fig. 4. Immune microenvironment analysis and potential drug prediction for biomarkers (**a**) Immune infiltration analysis, showing the expression differences of 55 immune cells in the AD and control groups of the training set. (**b**) Correlation heatmap of 55 differentially expressed immune cells. (**c**-**e**) Correlation analysis between biomarkers and differentially expressed immune cells. (**c**) CREBBP. (**d**) PIAS1. (**e**) TRIM28. (**f**) Biomarker-targeted drug network. Orange nodes represent mRNAs (biomarkers), and purple nodes represent targeted drugs.

of niacin and lysosome[37,38]. *PIAS1*, a protein inhibitor of the activated *STAT1*, is one of E3 the E3-type SUMO ligases. It plays important roles in the STAT pathway, which is essential to inflammatory activation in AD[39]. Besides that, *PIAS1* is thought to play a neuroprotective role against Aβ toxicity in AD[40,41] . *TRIM28* has also been demonstrated to be an E3 SUMOylation ligase[42]. Maxime et al. found that *TRIM28* regulates the steady state levels of a-Synuclein (a-Syn) and tau, which are supposed to be neurodegeneration-driving proteins in AD by mediating the SUMOylation[43,44]. The APOE ε4 allele, a major genetic risk factor for AD, contributes to pathogenesis through lysosomal dysfunction centered on transcription factor EB (TFEB). Studies have shown that defects exist downstream of calcineurin-activated TFEB cytoplasmic-to-nuclear translocation in patients with the APOE ε4/ε4 genotype[45]. Further research indicates that acetylation of TFEB is regulated by genes such as CREBBP[37], while deacetylation promotes lysosomal biogenesis in microglia and accelerates Aβ degradation[46]. Therefore, we hypothesize that SUMOylation-related genes such as CREBBP, PIAS1, and TRIM28 may cooperate with APOE ε4 to collectively disrupt proteostasis in AD by modulating the TFEB-mediated lysosomal pathway. However, the precise molecular mechanisms linking these SUMO regulatory factors to the APOE/TFEB axis await further experimental validation.

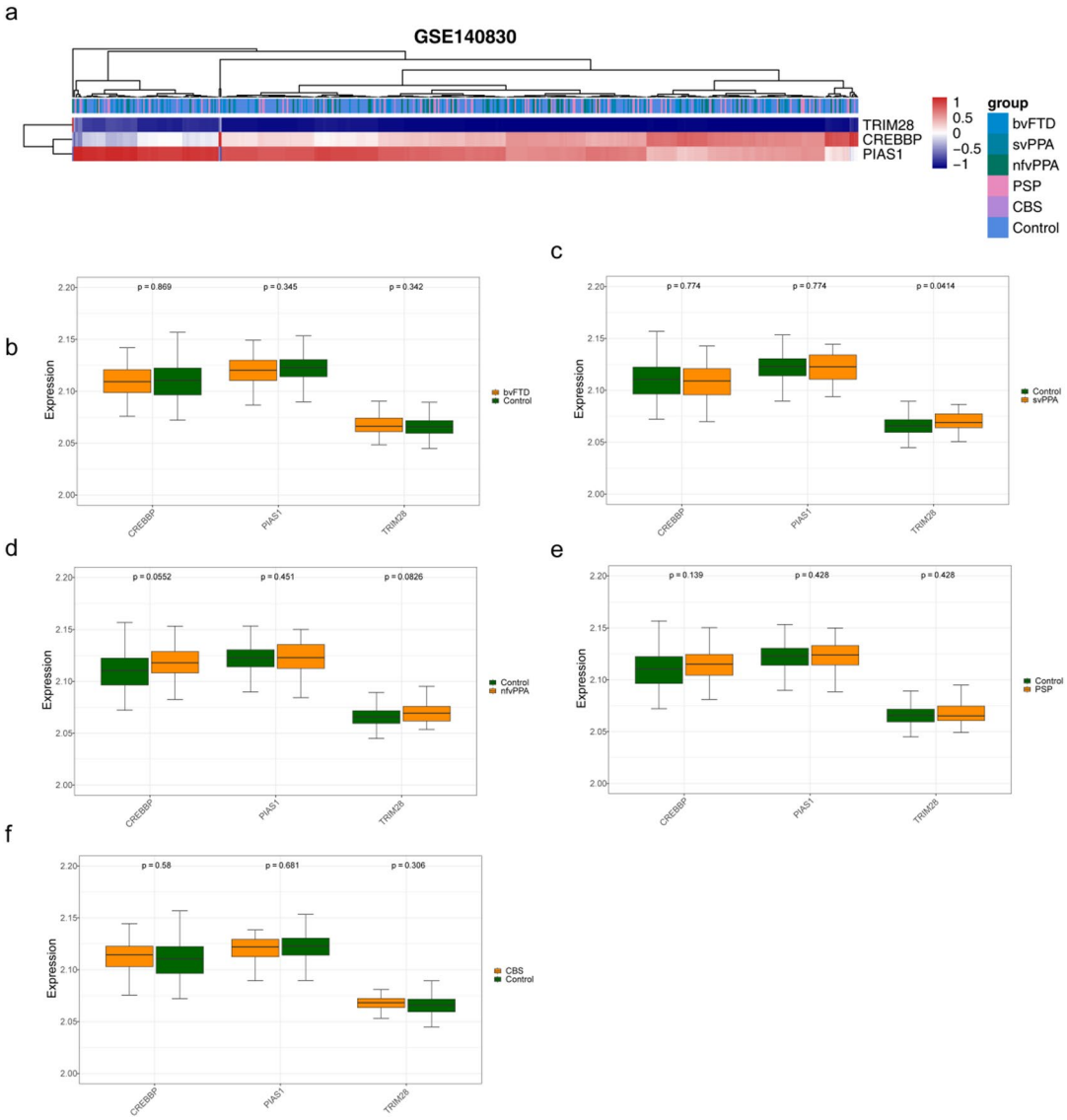

Fig. 5. Expression differences of biomarkers in different dementia-related diseases (**a**) Heatmap of biomarker expression in different dementia-related diseases. (**b**) Expression differences of biomarkers in bvFTD and control groups in GSE140830. (**c**) Expression differences of biomarkers in svPPA and control groups in GSE140830. (**d**) Expression differences of biomarkers in nfvPPA and control groups in GSE140830. (**e**) Expression differences of biomarkers in PSP and control groups in GSE140830. (**f**) Expression differences of biomarkers in CBS and control groups in GSE140830.

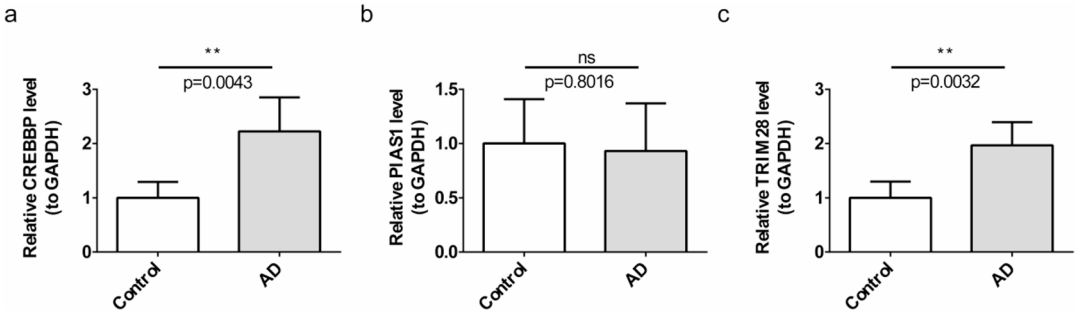

Fig. 6. Expression validation of key genes in clinical tissue samples, $p < 0.05$, ns, no significance (**a**) CREBBP. (**b**) PIAS1. (**c**) TRIM28.

GSEA showed that lysosome, olfactory transduction, and spliceosome are the pathways involved in these three biomarkers. Studies have shown that TRIM28 inhibits autophagy degradation by inducing SUMOylation of BCR-ABL[47]. Lysosomes are a significant cell signaling center, influencing fundamental processes such as cell membrane repair, energy metabolism, and inflammatory pathways[48]. The autophagy-lysosome pathway is closely related to protein homeostasis and other processes in AD[49]. Therefore, it is reasonable to speculate that the biomarker *TRIM28* may affect AD by participating in the regulation of the lysosomal pathway. Olfactory dysfunction often occurs in the early stages of AD, studies have found that the olfactory mucosal cells from AD patients secrete an increased amount of Aβ1-42, and the ratio of secretion of Aβ1-42 / Aβ1-40 also increases[50]. Splicing contributes to the diversity and function of neuronal transcription; the disruption of the splicing mechanism leads to neurological diseases, including AD[51]. Yi-Chen et al. supposed that the interaction of tau spliceosomes disrupts the function of snRNP, resulting in loss of transcriptome fidelity and splicing errors, and leading to neurodegenerative changes in AD ultimately[52].

The TF-mRNA indicated that *EGR1*, *DMRT1*, *CREM*, *ZFX*, and *E2F1* could simultaneously regulate three biomarkers. As a member of immediate early genes (IEGs), *EGR1* is a mediator and regulator of synaptic plasticity and neuronal activity under physiological conditions and in pathological conditions[53], and has recently been considered a candidate gene for schizophrenia. *CREM* and *CREB* are members of the same family of transcription factors, and *CREB* may have a significant effect on forming and consolidating of memory by interacting with *CREBBP*[54]. *ZFX* is a zinc finger protein of the Zfy family. David found that *ZFX* is a repressor of core and linker histones[55]. *E2F1* is a critical transcription factor regulating cell cycle, which is primarily considered to be a key factor in cell proliferation and cancer. Still, recent studies have suggested that it may also act as an important part in neurodegenerative diseases[56]. The expression levels of *E2F-1* in the brain tissue of AD model rats had changed, suggesting that *E2F-1* may be involved in neuronal death and loss of function by regulating cell cycle and apoptosis in AD[57]. These transcription factors associated with *CREBBP*, *PIAS1*, and *TRIM28* may mediate the development of AD by regulating histone acetylation, synaptic plasticity, and the cell cycle. However, the mechanisms of these effects still need to be further explored.

Neuroimmune interactions are a significant focus of research into neurodegenerative diseases, including AD, recently[58]. Our study found that in AD, the proportion of specific immune cells increased, such as basophils, class-switching memory B cells, muscle cells. In contrast, the proportion of specific immune cells decreased, such as natural killer T cells (NKT), B cells, neutrophils, smooth muscle, and naive CD8(+) T cells. The results are similar to previous studies[59,60]. In addition, among these immune cells, basophils were positively correlated with *PIAS1* and *CREBBP*, myocytes were positively associated with *TRIM28*, and there was a significant negative correlation between neutrophils with *CREBBP* and *PIAS1*, as well as smooth muscle and *TRIM28*. Basophils are a subset of granulocytes involved in various immunomodulatory and inflammatory processes. A study found that the number of basophils increased significantly in AD samples[61]. This is consistent with our findings, so we could speculate that *PIAS1* and *CREBB* may regulate the inflammatory response in AD by affecting neutrophils. However, Shad found blood levels of basophils were constantly low in AD[62], so the role of basophils in AD is still under more research. Similar to basophils, other types of cells have a complex relationship with this neurodegenerative disease. For example, myocytes also play an essential role in multiple physiological processes closely related to AD. Myocytes are mainly involved in muscle function, motor control, and energy metabolism. Cerebral small vessel disease (CSVD) is characterize with depletion of vascular myocytes, so vascular myocytes are considered as central to brain aging[63], and there is evidence that myocytes are the source of amyloid deposits in the meninges and cortical blood vessels[64], which may affect the progression of AD. SO *TRIM28* may participate in the pathological process of AD by affecting myocyte function and further increasing amyloid deposition in the brain. It is worth to noting that recent studies have suggested that blood–brain barrier (BBB) dysfunction is correlated with human cognitive impairment including the early stages of AD[56,65]. BBB is made up of various cell including smooth muscle cells, besides that, it has been suggested that neutrophils may be involved in the early development of AD by mediating BBB damage, intravascular adhesion, and invasion of the central nervous system[66]. Therefore, we speculated that these three biomarkers can mediates peripheral or central inflammatory processes and affect the integrity of BBB by affecting the function of immune cells, thereby contribute to the occurrence and development of AD.

Finally, we identified the potential therapeutic drugs targeting *CREBBP* through the DGIdb database, totally 21 drugs were screened including colchicine, glucocorticoid, benzodiazepines an so on, among which triazolam and alprazolam have been used to improve behavioral and psychological symptoms of AD[67]. As we know, although cholinesterase inhibitors, which designed to increase the levels of acetylcholine (ACh) in the brain, are the main drugs for AD, there are no therapeutic drugs with definite efficacy for AD[68]. Interestingly, Keisuke et al. recently founded that triazolam could inhibit rhAChE activity by ≥ 20%[69], which may provide new evidence for the use of benzodiazepines in the treatment of AD. In a word, our drug predictions based on these biomarkers, particularly those related to *CREBBP*, can provide valuable data for the exploit of more effective and safer AD drugs, but further research involving animal models and clinical trials is required to assess the safety and efficacy of these drugs.

Through systematic bioinformatic analysis, this study for the first time established *CREBBP, PIAS1*, and *TRIM28* as a SUMOylation-related biomarker panel for AD diagnosis. Although *PIAS1* did not reach statistical significance in the present clinical sample validation, it consistently showed a significant upregulation trend in two independent datasets, GSE140831 and GSE63060, and exhibited favorable diagnostic discriminative ability with an AUC exceeding 0.7 in the training set. It should be noted that the clinical validation in this study included only 5 pairs of AD and control samples, resulting in a relatively small sample size. This limitation may reduce statistical power, leading to a failure to detect truly existing differences, increase the risk of chance findings, and potentially restrict the representativeness of the results for the general population. Therefore, the lack of significantly differential expression of PIAS1 observed in this validation might be attributable to the

insufficient sample size rather than an inherent lack of diagnostic potential for this gene. Nevertheless, Thus, PIAS1 remains a promising peripheral blood biomarker for AD. Its lack of significant differential expression in this small-sample validation may be attributable to sample heterogeneity, dynamic expression changes, or assay sensitivity, warranting further validation in larger cohorts. More importantly, the nomogram diagnostic model constructed based on these three biomarkers demonstrated excellent comprehensive diagnostic performance (AUC > 0.8), suggesting that a "multi-gene panel strategy" offers greater robustness and clinical translation potential for early AD identification. This provides a new tool and perspective for non- or minimally invasive early diagnosis of AD. However, due to limitations in sample size and laboratory validation, the diagnostic efficacy and mechanistic roles of these SUMO-related gene markers require further confirmation. In the future, we will expand the cohort size, conduct multi-center clinical validation, and integrate proteomics and single-cell sequencing to systematically elucidate the regulatory network of this biomarker panel, optimize the diagnostic model, and promote its practical application in non-invasive early diagnosis of AD.

Conclusion

In conclusion, we identified CREBBP, PIAS1 and TRIM28 as SUMO-SRGs-based biomarkers diagnosing AD through bioinformatics analysis firstly in this study, furthermore, we revealed the regulatory networks and identified potential therapeutic agents aimed at these biomarkers. These genes may be involved in the onset and progression of AD, they have potential to be considered as novel biomarkers for AD's diagnosing and progression monitoring.

Data availability

The datasets analysed during the current study are available in the [GEO] repository, [https://www.ncbi.nlm.nih.gov/geo/, reference number GSE140831 (GPL15988), GSE63060 (GPL6947), GSE140830 (GPL15988)]. and [MSigDB] repository, [https://www.gsea-msigdb.org/]. The R code used in this study has been uploaded to the figshare repository platform and assigned the DOI: [https://doi.org/10.6084/m9.figshare.31861093]; readers may access it via this link.

Code availability

The R code used in this study has been uploaded to the figshare repository platform and assigned the DOI: [https://doi.org/10.6084/m9.figshare.31861093]; readers may access it via this link.

Received: 26 June 2025; Accepted: 17 April 2026
Published online: 20 April 2026

References

1. Arvanitakis, Z., Shah, R. C. & Bennett, D. A. Diagnosis and management of dementia: Review. *JAMA* **322**, 1589–1599. https://doi.org/10.1001/jama.2019.4782 (2019).
2. Scheltens, P. et al. Alzheimer's disease. *The Lancet* **397**, 1577–1590. https://doi.org/10.1016/S0140-6736(20)32205-4 (2021).
3. Barbe, C. et al. Factors associated with quality of life in patients with Alzheimer's disease. *BMC Geriatr.* **18**, 159. https://doi.org/10.1186/s12877-018-0855-7 (2018).
4. van der Lee, S. J. et al. The effect of APOE and other common genetic variants on the onset of Alzheimer's disease and dementia: A community-based cohort study. *Lancet Neurol.* **17**, 434–444. https://doi.org/10.1016/S1474-4422(18)30053-X (2018).
5. Rostagno, A. A. Pathogenesis of Alzheimer's disease. *Int. J. Mol. Sci.* **24**, 107. https://doi.org/10.3390/ijms24010107 (2022).
6. Passeri, E. et al. Alzheimer's disease: Treatment strategies and their limitations. *Int. J. Mol. Sci.* **23**, 13954. https://doi.org/10.3390/ijms232213954 (2022).
7. Martins, W. C., Tasca, C. I. & Cimarosti, H. Battling Alzheimer's disease: Targeting SUMOylation-mediated pathways. *Neurochem. Res.* **41**, 568–578. https://doi.org/10.1007/s11064-015-1681-3 (2016).
8. Grabbe, C., Husnjak, K. & Dikic, I. The spatial and temporal organization of ubiquitin networks. *Nat. Rev. Mol. Cell Biol.* **12**, 295–307. https://doi.org/10.1038/nrm3099 (2011).
9. Nortley, R. et al. Amyloid β oligomers constrict human capillaries in Alzheimer's disease via signaling to pericytes. *Science* **365**, eaav9518. https://doi.org/10.1126/science.aav9518 (2019).
10. Lee, L. et al. SUMO and Alzheimer's disease. *Neuromol. Med.* **15**, 720–736. https://doi.org/10.1007/s12017-013-8257-7 (2013).
11. Ciaffaglione, V. et al. SUMO-2 activity is inhibited by non-covalent interactions with the Aβ peptide: An exploration of potential pathogenic mechanisms in Alzheimer's disease. *Int. J. Biol. Macromol.* **323**, 146632. https://doi.org/10.1016/j.ijbiomac.2025.146632 (2025).
12. Mun, M.-J. et al. Polymorphisms of small ubiquitin-related modifier genes are associated with risk of Alzheimer's Disease in Korean: A case-control study. *J. Neurol. Sci.* **364**, 122–127. https://doi.org/10.1016/j.jns.2016.03.023 (2016).
13. Kuan, X.-Y., Fauzi, N. S. A., Ng, K. Y. & Bakhtiar, A. Exploring the causal relationship between telomere biology and Alzheimer's Disease. *Mol. Neurobiol.* **60**, 4169–4183. https://doi.org/10.1007/s12035-023-03337-4 (2023).
14. Zalzman, M. et al. The role of ubiquitination and SUMOylation in telomere biology. *Curr. Issues. Mol. Biol.* https://doi.org/10.21775/cimb.035.085 (2020).
15. Chang, B. et al. Development and validation of cuproptosis-related genes in synovitis during osteoarthritis progress. *Front. Immunol.* **14**, 1090596. https://doi.org/10.3389/fimmu.2023.1090596 (2023).
16. Ritchie, M. E. et al. Limma powers differential expression analyses for RNA-sequencing and microarray studies. *Nucleic Acids Res.* **43**, e47. https://doi.org/10.1093/nar/gkv007 (2015).
17. Pelikan, A., Herzel, H., Kramer, A. & Ananthasubramaniam, B. Venn diagram analysis overestimates the extent of circadian rhythm reprogramming. *FEBS J.* **289**, 6605–6621. https://doi.org/10.1111/febs.16095 (2022).
18. Kanehisa, M. KEGG: Kyoto encyclopedia of genes and genomes. *Nucleic Acids Res.* **28**, 27–30. https://doi.org/10.1093/nar/28.1.27 (2000).
19. Kanehisa, M. et al. KEGG as a reference resource for gene and protein annotation. *Nucleic Acids Res.* **44**, D457–D462. https://doi.org/10.1093/nar/gkv1070 (2016).
20. Wu, T. et al. clusterProfiler 4.0: A universal enrichment tool for interpreting omics data. *Innovation* **2**, 100141. https://doi.org/10.1016/j.xinn.2021.100141 (2021).

21. Shannon, P. et al. Cytoscape: A software environment for integrated models of biomolecular interaction networks. *Genome Res.* **13**, 2498–2504. https://doi.org/10.1101/gr.1239303 (2003).
22. Hu, X. et al. Combining metabolome and clinical indicators with machine learning provides some promising diagnostic markers to precisely detect smear-positive/negative pulmonary tuberculosis. *BMC Infect. Dis.* **22**, 707. https://doi.org/10.1186/s12879-022-07694-8 (2022).
23. Engebretsen, S. & Bohlin, J. Statistical predictions with glmnet. *Clin. Epigenetics* **11**, 123. https://doi.org/10.1186/s13148-019-0730-1 (2019).
24. Twait, E. L. et al. Dementia prediction in the general population using clinically accessible variables: A proof-of-concept study using machine learning. The AGES-Reykjavik study. *BMC Med. Inform. Decis. Mak.* **23**, 168. https://doi.org/10.1186/s12911-023-02244-x (2023).
25. Liu, T.-T. et al. Identification of CDK2-related immune forecast model and ceRNA in Lung adenocarcinoma, a pan-cancer analysis. *Front. Cell Dev. Biol.* **9**, 682002. https://doi.org/10.3389/fcell.2021.682002 (2021).
26. Liu, C. et al. Identification of novel potential homologous repair deficiency-associated genes in Pancreatic adenocarcinoma via WGCNA coexpression network analysis and machine learning. *Cell Cycle* **22**, 2392–2408. https://doi.org/10.1080/15384101.2023.2293594 (2023).
27. Goncharova, I. A. et al. Genetic predisposition to early myocardial infarction. *Mol Biol (Mosk)* **54**, 224–232. https://doi.org/10.31857/S0026898420020044 (2020).
28. Zhuang, X. et al. Time- and stimulus-dependent characteristics of innate immune cells in organ-cultured human corneal tissue. *J. Innate Immun.* **14**, 98–111. https://doi.org/10.1159/000516669 (2022).
29. Liu, S. et al. Identification of key circRNAs/lncRNAs/miRNAs/mRNAs and pathways in preeclampsia using bioinformatics analysis. *Med. Sci. Monit.* **25**, 1679–1693. https://doi.org/10.12659/MSM.912801 (2019).
30. Mangialasche, F. et al. Alzheimer's Disease: Clinical trials and drug development. *Lancet Neurol.* **9**, 702–716. https://doi.org/10.1016/S1474-4422(10)70119-8 (2010).
31. Hoppe, J. B., Salbego, C. G. & Cimarosti, H. SUMOylation: Novel neuroprotective approach for Alzheimer's disease?. *Aging Dis.* **6**, 322–330. https://doi.org/10.14336/AD.2014.1205 (2015).
32. Se Thoe, E. et al. A review on advances of treatment modalities for Alzheimer's Disease. *Life Sci.* **276**, 119129. https://doi.org/10.1016/j.lfs.2021.119129 (2021).
33. Cummings, J. L., Tong, G. & Ballard, C. Treatment combinations for Alzheimer's Disease: Current and future pharmacotherapy options. *J Alzheimers Dis JAD* **67**, 779–794. https://doi.org/10.3233/JAD-180766 (2019).
34. Goodman, R. H. & Smolik, S. CBP/p300 in cell growth, transformation, and development. *Genes Dev.* **14**, 1553–1577 (2000).
35. Schueller, E. et al. Dysregulation of histone acetylation pathways in hippocampus and frontal cortex of Alzheimer's Disease patients. *Eur. Neuropsychopharmacol.* **33**, 101–116. https://doi.org/10.1016/j.euroneuro.2020.01.015 (2020).
36. Jeong, H. et al. Acetylation targets mutant Huntingtin to autophagosomes for degradation. *Cell* **137**, 60–72. https://doi.org/10.1016/j.cell.2009.03.018 (2009).
37. Li, T. et al. TFEB acetylation promotes lysosome biogenesis and ameliorates Alzheimer's Disease-relevant phenotypes in mice. *J. Biol. Chem.* **298**, 102649. https://doi.org/10.1016/j.jbc.2022.102649 (2022).
38. Wang, Z., Zou, Z. & Li, Q. Nicotinic acid supplementation contributes to the amelioration of Alzheimer's disease in mouse models. *Ann. Transl. Med.* **10**, 1049. https://doi.org/10.21037/atm-22-1148 (2022).
39. He, K. et al. Functional genomics study of protein inhibitor of activated STAT1 in mouse hippocampal neuronal cells revealed by RNA sequencing. *Aging* **13**, 9011–9027. https://doi.org/10.18632/aging.202749 (2021).
40. Liu, S.-Y. et al. Protein inhibitor of activated STAT1 Ser503 phosphorylation-mediated Elk-1 SUMOylation promotes neuronal survival in APP/PS1 mice. *Br. J. Pharmacol.* **176**, 1793–1810. https://doi.org/10.1111/bph.14656 (2019).
41. Tao, C. C. et al. Epigenetic regulation of HDAC1 SUMOylation as an endogenous neuroprotection against Aβ toxicity in a mouse model of Alzheimer's disease. *Cell Death Differ.* **24**, 597–614. https://doi.org/10.1038/cdd.2016.161 (2017).
42. Neo, S. H. et al. TRIM28 is an E3 ligase for ARF-mediated NPM1/B23 SUMOylation that represses centrosome amplification. *Mol. Cell. Biol.* **35**, 2851–2863. https://doi.org/10.1128/MCB.01064-14 (2015).
43. Rousseaux, M. W. et al. Depleting Trim28 in adult mice is well tolerated and reduces levels of α-synuclein and tau. *Elife* **7**, e36768. https://doi.org/10.7554/eLife.36768 (2018).
44. Rousseaux, M. W. et al. TRIM28 regulates the nuclear accumulation and toxicity of both alpha-synuclein and tau. *Elife* **5**, e19809. https://doi.org/10.7554/eLife.19809 (2016).
45. Parcon, P. A. et al. Apolipoprotein E4 inhibits autophagy gene products through direct, specific binding to CLEAR motifs. *Alzheimers Dement.* **14**, 230–242. https://doi.org/10.1016/j.jalz.2017.07.754 (2018).
46. Bao, J. et al. Deacetylation of TFEB promotes fibrillar Aβ degradation by upregulating lysosomal biogenesis in microglia. *Protein Cell* **7**, 417–433. https://doi.org/10.1007/s13238-016-0269-2 (2016).
47. Liu, W. et al. Redox regulation of TRIM28 facilitates neuronal ferroptosis by promoting SUMOylation and inhibiting OPTN-selective autophagic degradation of ACSL4. *Cell Death Differ.* https://doi.org/10.1038/s41418-025-01452-4 (2025).
48. Lawrence, R. E. & Zoncu, R. The lysosome as a cellular centre for signalling, metabolism and quality control. *Nat. Cell Biol.* **21**, 133–142. https://doi.org/10.1038/s41556-018-0244-7 (2019).
49. Udayar, V., Chen, Y., Sidransky, E. & Jagasia, R. Lysosomal dysfunction in neurodegeneration: Emerging concepts and methods. *Trends Neurosci.* **45**, 184–199. https://doi.org/10.1016/j.tins.2021.12.004 (2022).
50. Lampinen, R. et al. Single-cell RNA-Seq analysis of olfactory mucosal cells of Alzheimer's disease patients. *Cells* **11**, 676. https://doi.org/10.3390/cells11040676 (2022).
51. Tollervey, J. R. et al. Analysis of alternative splicing associated with aging and neurodegeneration in the human brain. *Genome Res.* **21**, 1572–1582. https://doi.org/10.1101/gr.122226.111 (2011).
52. Hsieh, Y.-C. et al. Tau-mediated disruption of the spliceosome triggers cryptic RNA splicing and neurodegeneration in Alzheimer's Disease. *Cell Rep.* **29**, 301-316.e10. https://doi.org/10.1016/j.celrep.2019.08.104 (2019).
53. Duclot, F. & Kabbaj, M. The role of early growth response 1 (EGR1) in brain plasticity and neuropsychiatric disorders. *Front. Behav. Neurosci.* **11**, 35. https://doi.org/10.3389/fnbeh.2017.00035 (2017).
54. Bartolotti, N. & Lazarov, O. CREB signals as PBMC-based biomarkers of cognitive dysfunction: A novel perspective of the brain-immune axis. *Brain Behav. Immun.* **78**, 9–20. https://doi.org/10.1016/j.bbi.2019.01.004 (2019).
55. Gokhman, D. et al. Multilayered chromatin analysis reveals E2f, Smad and Zfx as transcriptional regulators of histones. *Nat. Struct. Mol. Biol.* **20**, 119–126. https://doi.org/10.1038/nsmb.2448 (2013).
56. Verdaguer E, Susana G de A, Clemens A, et al (2007) Implication of the transcription factor E2F-1 in the modulation of neuronal apoptosis. Biomed Pharmacother Biomedecine Pharmacother 61:390–399. https://doi.org/10.1016/j.biopha.2006.11.001
57. Tuerxun, M., Muhda, A. & Yin, L. The molecular mechanisms of signal pathway activating effect of E2F–1/NF-κB/GSK-3β on cognitive dysfunction of Alzheimer rats. *Bioengineered* **12**, 10000–10008. https://doi.org/10.1080/21655979.2021.1989261 (2021).
58. Jorfi, M., Maaser-Hecker, A. & Tanzi, R. E. The neuroimmune axis of Alzheimer's disease. *Genome Med.* **15**, 6. https://doi.org/10.1186/s13073-023-01155-w (2023).
59. Zhuang, X. et al. Development of a novel immune infiltration-related diagnostic model for Alzheimer's disease using bioinformatic strategies. *Front. Immunol.* **14**, 1147501. https://doi.org/10.3389/fimmu.2023.1147501 (2023).
60. Lu, Y., Li, K., Hu, Y. & Wang, X. Expression of immune related genes and possible regulatory mechanisms in Alzheimer's Disease. *Front. Immunol.* **12**, 768966. https://doi.org/10.3389/fimmu.2021.768966 (2021).

61. Johnson, M. D. & Blitman, J. Basophilic invasion in the neurohypophysis is increased in patients with Alzheimer's disease. *Clin. Neuropathol.* **39**, 271–274. https://doi.org/10.5414/NP301255 (2020).
62. Shad, K. F., Aghazadeh, Y., Ahmad, S. & Kress, B. Peripheral markers of Alzheimer's disease: Surveillance of white blood cells. *Synap N Y N* **67**, 541–543. https://doi.org/10.1002/syn.21651 (2013).
63. Ahmed-Jushuf, F. et al. Age-dependent expression of VEGFR2 in deep brain arteries in small vessel disease, CADASIL, and healthy brains. *Neurobiol. Aging* **42**, 110–115. https://doi.org/10.1016/j.neurobiolaging.2016.03.002 (2016).
64. Wisniewski, H. M., Wegiel, J. & Kotula, L. Review. David Oppenheimer Memorial Lecture 1995: Some neuropathological aspects of Alzheimer's disease and its relevance to other disciplines. *Neuropathol. Appl. Neurobiol.* **22**, 3–11. https://doi.org/10.1111/j.1365-2990.1996.tb00839.x (1996).
65. Van De Haar, H. J. et al. Blood-brain barrier leakage in patients with early Alzheimer disease. *Radiology* **282**, 615–615. https://doi.org/10.1148/radiol.2017164043 (2017).
66. Zenaro, E. et al. Neutrophils promote Alzheimer's disease–like pathology and cognitive decline via LFA-1 integrin. *Nat. Med.* **21**, 880–886. https://doi.org/10.1038/nm.3913 (2015).
67. Wang, F. et al. Drug therapy for behavioral and psychological symptoms of dementia. *Curr. Neuropharmacol.* **14**, 307–313. https://doi.org/10.2174/1570159X14666151208114232 (2016).
68. Lane, C. A., Hardy, J. & Schott, J. M. Alzheimer's disease. *Eur. J. Neurol.* **25**, 59–70. https://doi.org/10.1111/ene.13439 (2018).
69. Obara, K. et al. Inhibitory actions of antidepressants, hypnotics, and anxiolytics on recombinant human acetylcholinesterase activity. *Biol. Pharm. Bull.* **47**, 328–333. https://doi.org/10.1248/bpb.b23-00719 (2024).

Acknowledgements

This study was financially supported by the Intramural Research Project of Fuzhou Second General Hospital, China (Award Number: 2024ZY04), the Natural Science Foundation of Fujian Province, China (Award Number: 2023J011519), and the Natural Science Foundation of Fujian Province, China (Award Number: 2025J011378).

Author contributions

All authors contributed to the study conception and design. Peng Chen and Mengting Fan contributed equally to this work. Conceptualization:Peng Chen, Mengting Fan, Jing Xu; Methodology: Peng Chen; Formal analysis and investigation: Peng Chen; Writing—original draft preparation: Mengting Fan; Writing—review and editing: Peng Chen, Mengting Fan, Hailiang Lin, Zhong Chen, Qiuyang Zhang, Yunfan Cheng; Funding acquisition: Qiuyang Zhang, Jing Xu and Peng Chen.

Funding

This study was financially supported by the the Intramural Research Project of Fuzhou Second General Hospital, China (Award Number: 2024ZY04), the Natural Science Foundation of Fujian Province, China (Award Number: 2023J011519) and the Natural Science Foundation of Fujian Province, China (Award Number: 2025J011378).

Declarations

Competing interests

The authors declare no competing interests.

Ethics approval and consent to participate

This study was conducted in accordance with the Declaration of Helsinki. Ethical approval was obtained from the Ethics Committee of Fuzhou Second General Hospital, with the approval number 2024005 and the approval date February 29, 2024. All patients provided written informed consent when their clinical samples were used for RT-qPCR experiments, ensuring that the research process complied with ethical standards and fully respected the rights and wishes of the patients.

Consent for publication

Not applicable.

Additional information

Supplementary Information The online version contains supplementary material available at https://doi.org/10.1038/s41598-026-49884-3.

Correspondence and requests for materials should be addressed to J.X.